
Training neural networks to mimic the brain improves object recognition performance

Callie Federer

Department of Physiology and Biophysics
University of Colorado Anschutz Medical Campus
Aurora, CO
callie.federer@ucdenver.edu

Haoyan Xu

Department of Computing Science
University of Alberta
Edmonton, AB
haoyan5@ualberta.ca

Alona Fyshe

Department of Computing Science
University of Alberta
Edmonton, AB
alona@ualberta.ca

Joel Zylberberg

• Learning in Machines and Brains Program
Canadian Institute For Advanced Research (CIFAR)
Toronto, ON
joelzy@yorku.ca

Abstract

The current state-of-the-art object recognition algorithms, deep convolutional neural networks (DCNNs), are inspired by the architecture of the mammalian visual system, and capable of human-level performance on many tasks. However, even these algorithms make errors. As DCNNs train on object recognition tasks, they develop representations in their hidden layers that become more similar to those observed in the mammalian brains. Moreover, DCNNs trained on object recognition tasks are currently among the best models we have of the mammalian visual system. This led us to hypothesize that teaching DCNNs to achieve even more brain-like representations could improve their performance. To test this, we trained DCNNs on a composite task, wherein networks were trained to: a) classify images of objects; while b) having intermediate representations that resemble those observed in neural recordings from monkey visual cortex. Compared with DCNNs trained purely for object categorization, DCNNs trained on the composite task had better object recognition performance, make more reasonable errors and are more robust to label corruption. Our results outline a new way to train object recognition networks, using strategies in which the brain serves as a teacher signal for training DCNNs.

1 Introduction

Deep convolutional neural networks (DCNNs) have recently led to a rapid advance in the state-of-the-art object recognition systems [13]. At the same time, there remain critical shortcomings in these systems [15]. We asked whether training DCNNs to respond to images in a more brain-like manner could lead to better performance. Motivating us, DCNN architectures are directly inspired by that of the mammalian visual system (MVS) [6], and as DCNNs improve at object recognition tasks, they learn representations that are increasingly similar to those found in the MVS [8, 20, 4, 14]. Consequently, we expected that forcing the DCNNs to have image representations that were *even more* similar to those found in the MVS, could lead to better performance.

Previous work showed that the performance of smaller “student” DCNNs could be improved by training them to match the image representations of larger “teacher” DCNNs [14, 16, 5], and that DCNNs could be directly trained to reproduce image representations formed by the V1 area of

monkey visual cortex [7]. These studies provide a foundation for the current work, in which we used monkey V1 as a teacher network for training DCNNs to categorize images. We refer to the monkey V1 as the “teacher” for our DCNNs. DCNNs trained with the monkey V1 as a teacher outperformed those trained without this teacher signal, by several relevant metrics. This provides a proof of concept that the brain can be used as a teacher, to improve machine learning systems for vision-based tasks.

Notably, for this proof-of-concept study, we did not aim to achieve state-of-the-art classification performance: we used neural networks that are small relative to the current state-of-the-art (the largest networks we considered have the VGG-16 architecture). However, our results indicate that, even for moderately powerful DCNNs, (1) DCNNs trained to mimic monkey V1 have better object recognition performance, (2) DCNNs trained to mimic monkey V1 make more reasonable errors and (3) DCNNs trained to mimic monkey V1 are more robust to label corruption. We anticipate that future studies could apply this training method to larger networks, thereby improving on the current state-of-the-art object recognition systems.

2 Methods

2.1 Monkey Visual Cortex Data

Our monkey V1 teacher signal is from publicly-available multielectrode recordings from anesthetized monkeys presented with a series of images while experimenters recorded the spiking activity of neurons in primary visual cortex (V1) with a multielectrode array [2]. These recordings were conducted in 10 experimental sessions with 3 different animals, resulting in recordings from 392 neurons. The monkeys were shown 270 static natural images as well as various static grating images for 100 ms presentations.

2.2 Representational Similarity Matrices (RSMs)

To compare image representations in the monkey brain with those in a DCNN, we used representational similarity matrices (RSMs) as the teacher signal [9]. For each pair of images (i & j) shown to the monkey, we computed the similarity between measured neural responses (v_i & v_j): these vectors contain the firing rates of all of the observed neurons. We measured the similarity using the cosine similarity between those vectors (Fig. 1). These values (RSM_{ij}) were assembled into matrices, describing the representational similarities [9] in monkey V1, for all image pairs (i & j). We averaged the representational similarity matrices over the 10 experimental sessions to yield a single RSM that was used for training the neural networks. During DCNN training, we input the same pairs of images (i & j) into our DCNNs as were displayed to the monkeys, and computed representational similarity matrices for the chosen layer of hidden units (Fig. 1): the DCNN’s RSM is denoted by \widehat{RSM} .

2.3 Deep Convolutional Neural Networks and Cost Functions

We performed most of our experiments on the CORNet-Z DCNN architecture, described below. We also performed some experiments on the larger VGG-16 architecture. Results were similar for both architectures. The CORNet-Z DCNN architecture [12] is a trimmed-down version of the AlexNet [10] object recognition algorithm (Fig. 1). The layers in CORNet-Z have been identified with the brain areas at the corresponding depths within the mammalian visual hierarchy [12] (Fig. 1). We trained the networks on the CIFAR100 [11] task, which consists of classifying images of objects from 100 different categories. Regardless of the network architecture, we randomly initialized all weights with the Glorot uniform initializer [3], and trained the DCNN to minimize a cost function consisting of two terms: classification error, and mismatch between the network’s hidden representations and those in monkey V1. Classification error was computed as the cross entropy between the network’s final outputs and the true object labels. Representation mismatch was computed as the mean-squared error between the monkey V1 representational similarity matrix (RSM), and that of the relevant layer of the DCNN (\widehat{RSM}). For CORNet-Z, this was the V1 block (Fig. 1), and for VGG-16, this was the third convolutional layer. That layer was chosen because, in VGG-16 networks trained for object recognition tasks, it has representations most similar to those seen in monkey V1 [1].

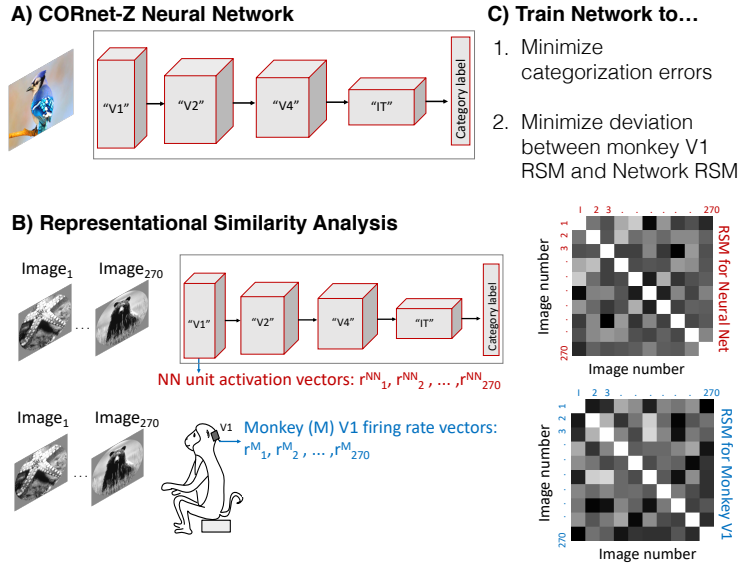


Figure 1: We did the majority of our experiments using the CORNet-Z architecture; some of our experiments were also done using the larger VGG-16 architecture (not shown). A) CORNet-Z has multiple blocks, each of which consists of a convolution followed by a ReLU nonlinearity and max pooling. The blocks are identified with cortical areas V1, V2, V4 and IT, which exist at the corresponding depths in the primate visual system. B) To compare the neural network’s image representation to that of monkey V1, we used a set of 270 images that were shown to monkeys while firing rates were recording using an implanted Utah array. We input each of these images to the artificial neural network, and extracted the vectors of unit activations in the network’s V1 layer. We then computed the representation similarity matrix (RSM) for the neural network; this 270 x 270 matrix defines how similar the unit activation patterns in the network are, for each image pair. We also computed the representation similarity matrix for monkey V1, over the same set of 270 images. C) We trained the neural networks to minimize errors in categorizing CIFAR100 images, while also minimizing the differences between their RSMs, and the one observed in monkey V1.

A trade-off parameter, λ , determines the relative weighting of the two terms in the cost function

$$cost = \lambda \sum_{i,j} (RSM_{ij} - \widehat{RSM}_{ij})^2 - \sum_i \hat{y}_i \log(y_i). \quad (1)$$

We updated the trade-off parameter λ throughout training, so as to keep the ratio between the two terms in the loss function constant. In other words, λ was updated so that r was constant, with $r = \lambda \left[\sum_{i,j} (RSM_{ij} - \widehat{RSM}_{ij})^2 \right] / \left[\sum_i \hat{y}_i \log(y_i) \right]$. We studied networks with several different values of this ratio, r . We also experimented with using a constant λ throughout training but found this constant-ratio method leads to better object recognition performance (Fig. A.1).

2.4 Training Procedures

We trained each CORNet-Z network for 100 epochs (250 for VGG-16, discussed in sec. 3.7). Networks trained with neural data (i.e., with $r > 0$), were trained to minimize the composite cost (Eq. 1) for the first 10 epochs, and thereafter were trained on just the cross entropy loss (this increased from 10 to 100 epochs for the VGG-16 experiments). In other words, we set $r = 0$ after these first 10 epochs, meaning there would be no training from the monkey V1 “teacher signal”. This procedure reduces the computational cost due to computing the representational similarity with two separate forward passes, one with the natural images from the monkey experiments and one with the CIFAR100 data. We performed some experiments in which the neural data regularizer was applied at all training epochs, and saw similar results (Fig. A.2).

We kept a static training rate of 0.01 for all networks and a batch size of 128 for CORNet-Z or 256 for VGG-16. We used dropout regularization [18] with 0.5 retention probability for the 3 fully connected layers of all networks. For the training images, we centered the pixels globally across channels. The held-out testing images were not preprocessed, to ensure fair evaluation. The natural images that were presented to the monkeys in the neuroscience experiments were also not preprocessed. The trained network weights, and code associated with this paper, can be downloaded at github.com/cfederer/TrainCNNsWithNeuralData.

For each architecture and choice of parameters, we repeated the training from 10 different random initial conditions; results reported are mean \pm SEM. This approach has a larger computational cost than does reporting the result of a single training run, but makes it more likely that our findings will generalize because they do not depend on the idiosyncrasies of weight initializations.

2.5 Control Experiments with Randomly Generated RSMs

For control experiments, we tested whether randomly generated RSMs would have the same benefit in object recognition performance as the monkey V1 RSMs. We repeated our experiments with randomly-generated RSMs in place of the monkey V1 ones. We generated the random RSMs in several different ways.

First, we drew 39-element i.i.d. random vectors from a Gaussian distribution with the same mean and variance as were seen in the monkey data: $\mu = 0.495$ and $\sigma = 0.582$; different random vectors were drawn for each image. We then used these random vectors to generate a RSM, as described above. This RSM is referred to as "Gaussian (V1-stats)". The number of elements (39) matches the average number of neurons simultaneously observed in the monkey experiments [2].

To test whether matching the statistics of the neural data matters for training the networks, we next drew 39-element vectors from i.i.d. Gaussian distributions with $\mu = 5$ and $\sigma = 0.582$, and calculated the representational similarity matrix from these randomly drawn vectors. This RSM is referred to as "Gaussian (non V1-stats)" because its mean (and mean-variance relationship) differ substantially from the neural data.

Finally, we applied a shuffling procedure to the V1 data, where we randomly permuted the image identities associated with each recorded vector of neural firing rates. As a result of this procedure, the neural responses no longer matched the images that were shown to the monkey. The random permutation was done independently for each neuron. This leads to vectors of firing rates that match (for each neuron, and to all orders) the distributions seen in the monkey data, but removes information about the specific image features those neurons represent (i.e., the neurons' receptive fields). Similar to the above experiments, we assembled these vectors into a RSM. This RSM is referred to as "V1 shuffled".

3 Results

We trained neural networks on the composite cost (Eq. 1), with varying ratios r describing the trade-off between representational similarity cost and categorization cost. We evaluated the trained networks based on categorization accuracy achieved on held-out data (not used in training) from the CIFAR100 dataset. In our figures, black lines indicate networks trained purely for categorization ($r = 0$), while red lines indicate networks trained using monkey V1 as a teacher ($r > 0$; see Methods). Higher weightings of neural data in the loss function correspond to darker red lines.

3.1 Networks trained to to Mimic Monkey V1 Image Representations Have Higher Object Recognition Accuracy

We first present results from the CORNet-Z architecture, and we discuss results from the larger VGG-16 model in Sec. 3.7. We tested the trained models' ability to classify previously-unseen images from the CIFAR100 dataset (i.e., images not used in training), and quantified the fraction of images correctly labeled. Networks trained to both classify objects and match neural representations (i.e., those with $r > 0$) can have better object recognition performance than those trained without using the monkey brain as a teacher (i.e., those with $r=0$; Fig. 2). The effect is not monotonic: maximum object recognition performance is achieved with $r = 0.1$; larger values of r lead to a

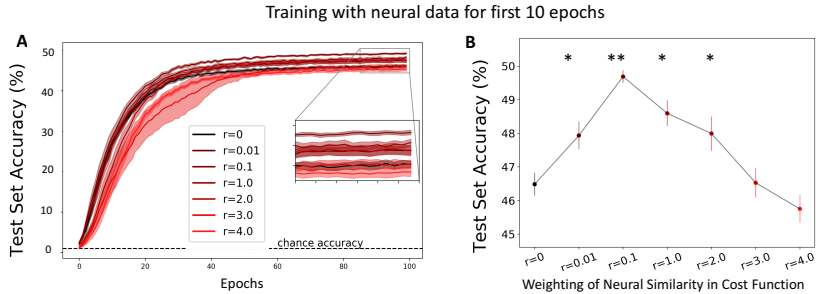


Figure 2: Accuracy in categorizing previously-unseen CIFAR100 images for the CORNet-Z architecture trained with different weighting ratios, r , applied to monkey V1 representation similarity for the first 10 epochs of training. A) Test-set accuracy at each epoch during training. Chance accuracy indicated by dashed black line. Shaded areas are \pm SEM over 10 different random initializations of each model. B) Test-set accuracy for previously-unseen CIFAR100 images at the end of training, as a function of the weight (r) given to neural representational similarity in the cost function. Double asterisks (**) indicate significantly higher results from no neural data, $r = 0$, at $p < .001$ on a one-tailed t-test. Single asterisks (*) indicate significantly higher results from no neural data, $r = 0$, at $p < .05$ on a one-tailed t-test.

reduction in object recognition performance, presumably because the training procedure places an insufficient emphasis on categorization (e.g., cross entropy).

3.2 Networks trained to to Mimic Monkey V1 Image Representations Have More Diverse Unit Activations

What is different in the V1-like layers of the networks trained with neural data? To gain insight into this question, we used t-SNE [19] to visualize the unit activations from the first convolutional layer of the networks from the preceding section (i.e., the layer of CORNet-Z that aligns with monkey V1 in terms of depth in the visual pathway). We input images from the CIFAR100 test set into the networks, and used t-SNE to embed those network activations into two dimensions. We repeated this procedure for networks trained with no monkey V1 teacher signal, $r = 0$, and with monkey V1 teacher signal, $r = 0.1$.

While the representations of images from different categories remain co-mingled at this low level of the neural network, the representations are more varied for the network trained with a neural representation weighting of $r = 0.1$ (Fig. 3b) than for the network trained no neural data ($r = 0$; Fig. 3a). This motivated us to compute the average variance per unit within the V1-like layer of the CORNetZ networks (variance in activations over the test-set images, averaged over all units in that hidden layer). As the weighting ratio r of neural similarity in the cost function increases, so too does the activation variance (Fig. 3c). While this increase in activation variance is initially associated with increasing object-recognition performance (e.g., up to $r = 0.1$), at higher values of r , that increased unit activation variance no longer correlates with higher accuracy (e.g., for $r = 3.0$ or $r = 4.0$; Fig. 3c). These data suggest that the improved generalization performance obtained by using neural data in the training procedure (i.e., Fig. 2) could arise in part because the training procedure that uses neural data forces the networks to have more diverse activations in their low-level units. Variance in activations alone does not explain the increase in categorization performance.

3.3 The Details of the “Teacher” Representation Matter

Training neural networks to categorize objects, while mimicking the image representations seen in monkey V1, leads to improved object recognition performance (Fig. 2). Is that result specific to the image representations in the monkey brain, or would having *any* arbitrary added RSM constraint in the cost function yield similar results? To answer this question, we performed the same neural network experiment described above (Fig. 2), but using randomly generated matrices in place of the monkey V1 representational similarity matrices. For these experiments, we used the optimal cost

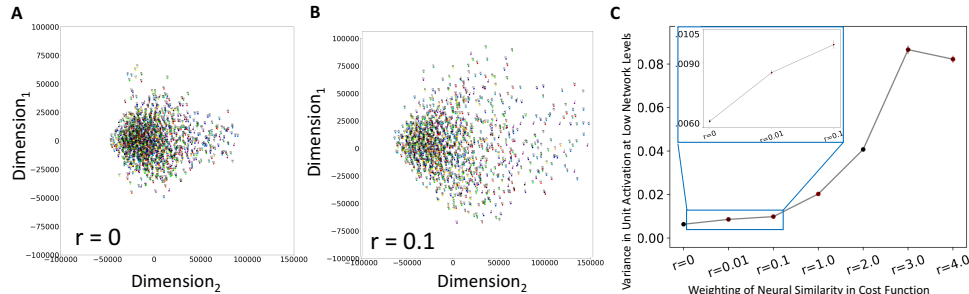


Figure 3: Visualizing the hidden unit activations. In panels A and B, we input the same 1280 randomly-selected images from the CIFAR100 test set into DCNNs trained with either $r = 0$ or $r = 0.1$. We then used t-SNE to embed those high-dimensional unit activations into two dimensions. X- and Y-axes represent the two dimensions of this t-SNE embedding. Colors indicate the object categories for each input image. A) t-SNE embedding of hidden-unit activations from networks trained with no neural data ($r = 0$). B) t-SNE embedding of hidden-unit activations from networks trained with neural data $r = 0.1$ for the first 10 epochs of training. C) Average variance per unit in the V1-like layer of trained CORNet-Z networks with different weightings, r , of neural representations in the cost function. Inset zooms in on the first data points for $r = 0, 0.01, 0.1$. It is important to note that the exact outcome of the t-SNE embedding is sensitive to differences in settings.

function weighting ratio, r , found from our experiments with V1 data: $r = 0.1$. We repeated these experiments with $r = 0.01$ and $r = 1.0$ and found similar results (Fig. A.3).

We created randomly-generated RSMs in several different ways (see Methods), used them in place of the monkey V1 RSM teacher signal in the training procedure, and compared the trained networks' object categorization performance. Networks trained with the randomly generated RSMs (either with or without matching the mean of the monkey data) under-performed ones trained with real V1 data for the teacher RSM. Networks trained with shuffled V1 data get nearly the same testing accuracy as do those trained with real V1 data (Fig. 4), although the real V1 data still appears to form (by a small margin) the best teacher representation. The teacher RSM may be instructing the DCNN about the distribution of activations (see Sec. 3.2), making the statistics of the data important while not requiring the exact V1 data. These results demonstrate that regularization effects alone – forcing the network to match an arbitrary RSM – results in worse performance than when the “teacher” RSM has statistical properties similar to those seen in V1. We did not do a full search of drawing from Gaussian distributions with varying mean and standard deviation. Future work could systematically determine at which point the Gaussian-drawn RSM values are no longer close enough to the neural data to be useful.

3.4 The Layer of Representation Teaching Matters

Above, we found that the details of the RSM used as a teacher for training the DCNN, matter. This led us to wonder whether it matters *where* in the network that representational similarity cost is applied. To test this, we repeated the experiments from Fig. 2 (training CORNet-Z architecture DCNNs with different weightings for the mismatch between network RSM and monkey V1 RSM), but computed the representation similarity cost for layers other than the V1-identified CORNet-Z layer. The resultant networks all had lower training and testing accuracy than did networks trained with no neural data (Fig. A.4). These results, and those in the preceding section, demonstrate that the performance benefits of the monkey V1 representation teacher require that the monkey V1 representation similarity cost be assigned to the appropriate (early) layer in the DCNN.

3.5 Networks trained to to Mimic Monkey V1 Image Representations Make More-Sensible Errors

We demonstrated that teaching neural networks to respond to images in a more brain-like manner boosts accuracy in categorizing held-out testing data (Fig. 2). All networks, regardless of regulariza-

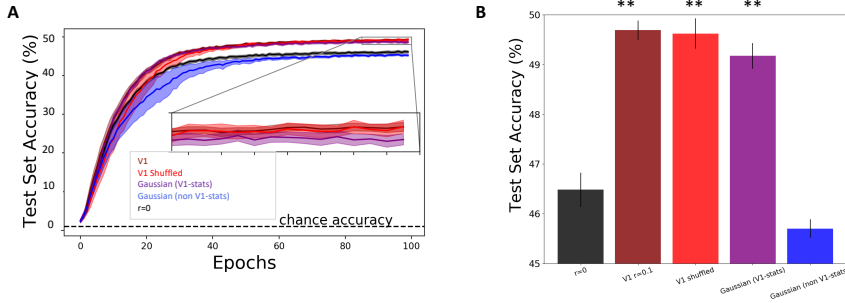


Figure 4: Accuracy in categorizing previously un-seen CIFAR100 images for networks trained with different teacher RSMs: the real monkey V1 RSM (dark red); V1 shuffled RSM (light red); RSM from random Gaussian vectors drawn with the same mean and standard deviation as the V1 data (Gaussian V1-stats in purple); and RSM from random Gaussian vectors drawn with different mean than the neural data (Gaussian non V1-stats in blue). These were all trained with a weighting of $r = 0.1$ applied to the representational similarity in the loss function. For comparison, the baseline network (trained with no representational similarity cost) is shown in black. A) Testing accuracy over epochs of training. Shaded areas on plot are \pm SEM over 10 different random initializations of each model. B) Test accuracy plotted (same as in A) by type of data used in forming the teacher RSM. Lines on bars are \pm SEM over 10 different random initializations of each model. Double asterisks (**) indicate significantly higher results from no neural data, $r = 0$, at $p < .001$ on a one-tailed t-test. Single asterisks (*) indicate significantly higher results from no neural data, $r = 0$, at $p < .05$ on a one-tailed t-test.

tion, still make frequent errors. However, some errors are worse than others. For example, confusing a mouse for a hamster is more reasonable than confusing a mouse for a skyscraper. This intuition led us to quantify the quality of the errors made by each of our trained networks. For this purpose, we exploited the fact that the 100 classes of labels in the CIFAR100 dataset are grouped into 20 superclasses. One example is “small mammals”, which encompasses mouse, squirrel, rabbit and shrew.

We thus asked, for each trained network, what fraction of their categorization errors were within the correct superclass (e.g., confusing a hamster for a mouse) vs in the wrong superclass (e.g., confusing a mouse for a skyscraper). We performed this test on the network trained with the monkey V1 data as a teacher, with the weighting ratio that yielded the best categorization performance ($r = 0.1$). For this network, errors were within the correct superclass 23.9% of the time (Fig. 5, Table 1). For comparison, for the network trained with no neural data, errors were within the correct super class 22.8% of the time (Fig. 5, Table 1).

Networks trained to categorize images, while using monkey V1 as a teacher make fewer categorization errors (Fig. 2). When they do make errors, those errors are more often within the correct superclass and thus more reasonable (Fig. 5, Table 1). We find a similar pattern in networks trained with other weighting ratios r (Table 1). Moreover, results with randomly generated RSMs mirror their impact on categorization: training with a teacher RSM results both in improved accuracy and an increase in the fraction of errors that are within the correct superclass.

Table 1: The percentage of errors that are within the correct superclass in the CIFAR100 dataset.

Weighting of Neural Similarity in Cost Function	Regularization Data	Errors Within Correct Super Class(%) \pm SEM
$r=0$	None	22.8% \pm 0.002
$r=0.1$	V1	23.9% \pm 0.002
$r=0.1$	V1 Shuffled	23.9% \pm 0.001
$r=0.1$	Gaussian (V1-stats)	23.7% \pm 0.001
$r=0.1$	Gaussian (non V1-stats)	22.6% \pm 0.002

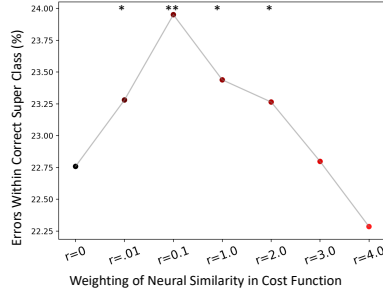


Figure 5: Percentage of errors within the correct superclass for networks trained with the monkey V1 RSM as a teacher, and various weightings of neural similarity in the cost function (Eq. 1). Double asterisks (**) indicate significantly higher results from no neural data, $r = 0$, at $p < .001$ on a one-tailed t-test. Single asterisks (*) indicate significantly higher results from no neural data, $r = 0$, at $p < .05$ on a one-tailed t-test.

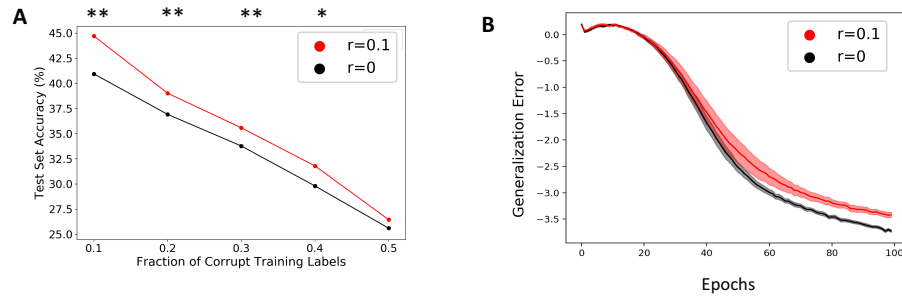


Figure 6: Training CORNet-Z networks with corrupted labels. A) Test set accuracy on networks trained with (red) and without (black) neural data, with different fractions of corrupted labels in the training set. Labels for the test set were not corrupted. Double asterisks (**) indicate significantly different results from no neural data, $r = 0$, at $p < .001$ on a one-tailed t-test. Single asterisks (*) indicate significantly higher results from no neural data, $r = 0$, at $p < .05$ on a one-tailed t-test. B) Generalization error (training loss - testing loss) on networks trained with (red) and without (black) neural data and different fractions corrupted training labels. Line patterns indicate different fractions of corrupted labels in the training set. Shaded areas are \pm SEM over 10 different random initializations of each model.

3.6 Networks trained to Mimic Monkey V1 Image Representations are More Robust to Label Corruption

Given that networks trained using neural data made fewer, and more reasonable, errors, we hypothesized that they generalized more robustly. To test that hypothesis, we performed experiments in which some image labels in the training dataset were incorrect. Datasets will often contain mislabeled images, and ideally computer vision networks would not be heavily affected by these. To generate a corrupted training set, we shuffled labels of 10% to 50% of the training dataset, keeping the distribution of classes equal. We only corrupted the training data, and left testing data intact. We then trained CORNet-Z networks with $r = 0.1$, and networks without neural data, $r = 0$. By the end of the 100 training epochs, networks trained with neural data achieved better testing accuracy than did those without neural data (Fig. 6B). The generalization error (training loss - testing loss) was also lower for networks trained with neural data (Fig. 6C). Networks trained with neural data are more robust to mislabeled images than those trained without neural data.

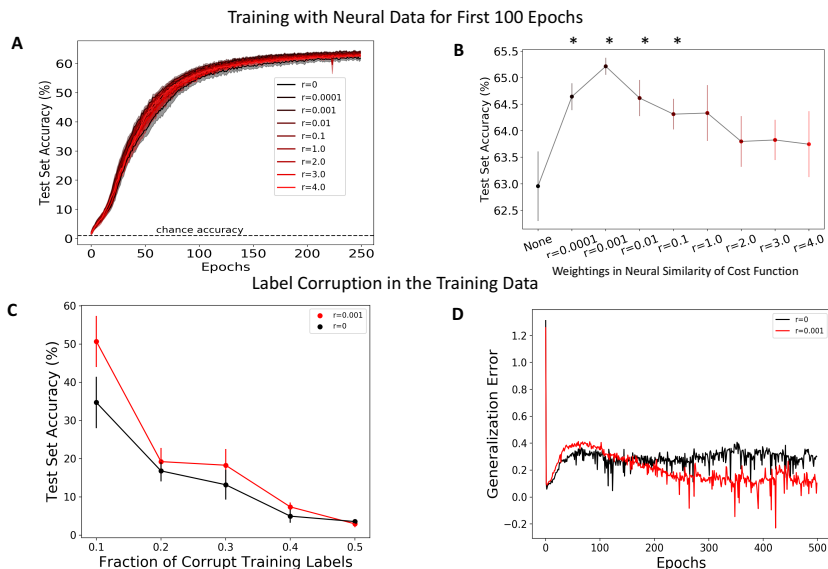


Figure 7: Accuracy in categorizing previously-unseen CIFAR100 images for the VGG-16 architecture trained on the composite tasks, with different weighting ratios, r , applied to monkey V1 representational similarity in the cost function. A) Testing accuracy for each epoch of training. Chance accuracy indicated by dashed black line. Shaded areas on plot are \pm SEM over 10 different random initializations of each model. B) Test accuracy plotted (same as in A) vs the weight of the emphasis on neural representation similarity. Single asterisks (*) indicate significantly higher results from no neural data, $r = 0$, at $p < .05$ on a one-tailed t-test. C) Test set accuracy on networks trained with (red) and without (black) neural data, with different fractions of corrupted labels in the training set. Labels for the test set were not corrupted. D) Generalization error (training loss - testing loss) on networks trained with (red) and without (black) neural data and 0.1 fraction corrupted training labels.

3.7 Similar Results are Obtained with the Larger VGG-16 Network

All of the above experiments were run with the relatively small CORNet-Z network. This led us to wonder whether monkey V1 data could serve as a similarly effective teacher for deeper neural networks with higher baseline performance. To answer this question, we repeated our above experiments, but using the VGG-16 architecture [17] in place of CORNet-Z. We applied the monkey V1 representational similarity cost at the third convolutional layer of the VGG-16 (see Methods). We found that, with the VGG-16 architecture, the monkey V1 teacher signal improves categorization performance, increases robustness to corrupted labels in the training set, and reduces generalization error, similar to what was observed with the smaller CORnet-Z architecture (Fig. 7).

4 Discussion

Training the early layers of convolutional neural networks with to mimic the image representations from monkey V1 improves those networks' ability to categorize previously-unseen images. Moreover, networks trained in this manner, using monkey V1 as a representation "teacher" made errors that were more reasonable than did networks that were not trained to mimic monkey V1. These results were consistent for two different network architectures of vastly different sizes (CORNet-Z and VGG-16), suggesting that they will generalize well to other networks.

Our experiments indicate that the distributions of activations for the "teacher" representation are important: making the earlier layers of the neural network have V1-like activation distributions is helpful for categorization performance. Important future work will be needed to determine if having actual neural data makes a large difference: we found that image-shuffled shuffled neural data ("V1 shuffled") worked almost as well. It is important to note that the data we used here were from anesthetized monkeys, who were shown the images for very brief periods (100 ms). Moreover, with the recording method used (Utah arrays implanted in V1), only O(10) neurons could

be simultaneously observed. Despite the caveats of our dataset, we found that the statistically closer the teacher representation was to the real neural data, the better the trained neural network did at object recognition. A key future direction – that we are actively pursuing – is to repeat the experiments here, but with data from awake animals, doing vision-based tasks, in which a larger fraction of V1 is observed.

We emphasize that our goal was not to achieve state-of-the-art classification performance, but rather to determine whether and how we could use the brain as a teacher for training artificial neural networks to perform object recognition tasks. We tested this with powerful but relatively small networks. We have demonstrated proof-of-concept that using the brain as a teacher signal results in better performance, leaving for future work the important tasks of optimizing hyperparameters like learning rate, and applying this neural data teaching procedure to larger networks. Our expectation is that such work will yield better object recognition systems.

Appendix

A.1 Training With Static Cost Weightings

In the experiments in the main paper, we adjusted the weighting of the representation similarity cost in the loss function (λ) during training, so as to keep a constant ratio (r) between the cross-entropy cost and the representation similarity cost. We also applied the representation similarity cost only for the first 10 epochs of training. A natural question is whether similar results would be achieved with a static λ value, or with the representation similarity cost applied for longer durations during training. To answer this question, we repeated our experiments from Fig. 2, with static λ values, and with $\lambda \neq 0$ for the first 100 epochs of training (instead of 10). We found that this method did not work as well as the one described in Fig. 2: to see this, compare the accuracy values in Fig. 2 to those in Fig. A.1.

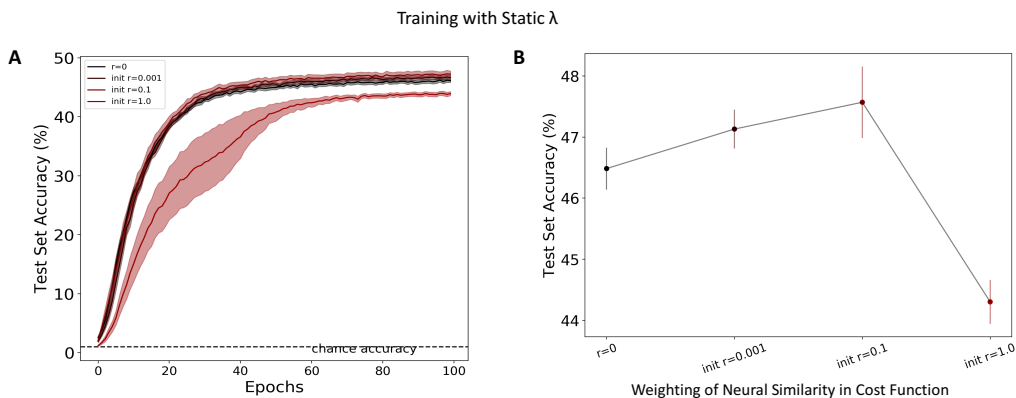


Figure A.1: Accuracy in categorizing previously-unseen CIFAR100 images for the CORNet-Z architecture trained with different initial weighting ratios, $init\ r$, applied to monkey V1 representation similarity for all 100 epochs of training. The test-set accuracy is plotted at each epoch during training. Chance accuracy indicated by dashed black line. Shaded areas are \pm SEM over 10 different random initializations of each model. B) Test-set accuracy for previously-unseen CIFAR100 images at the end of training, as a function of the initial static weight, $init\ r$, given to neural representational similarity in the cost function.

A.2 Training Over Longer Timescales

In the main paper, we used the neural data regularizer only during the first 10 epochs of the training procedure: after the 10th epoch, the weighting parameter, r , was set to zero. This led us to wonder whether larger performance benefits might be obtained by extending the time window over which the neural data contributed to the training. To answer this question, we trained networks with neural data for all 100 epochs, instead of the first 10, and found a similar boost in testing accuracy for

networks trained with neural data (Figs. A.2 A, B). This demonstrates that we do not need to run the regularization step for longer than the first 10 epochs.

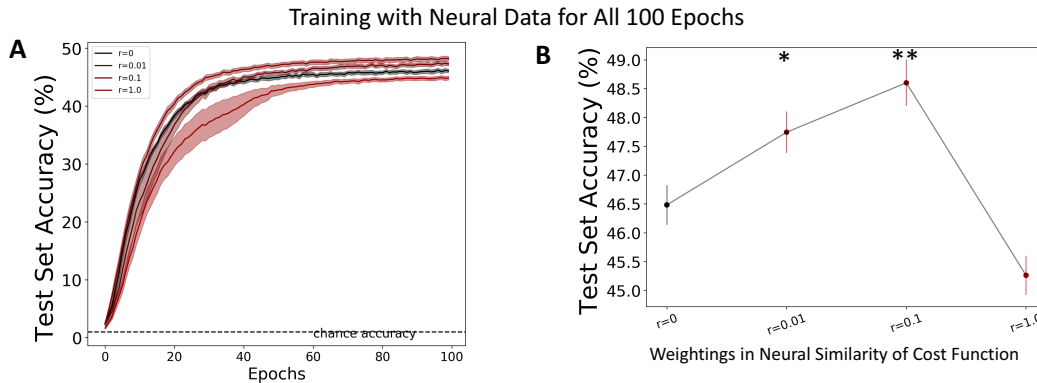


Figure A.2: Training with representation similarity cost at all epochs. (Similar to Fig. 2 but with representation similarity cost applied for all 100 epochs). A) Testing accuracy for each epoch of training with static weighting ratio, r . B) Test accuracy (same as in A) vs the weight of the emphasis on neural representation similarity. Double asterisks (**) indicate significantly higher results from no neural data, $r = 0$, at $p < .001$ on a one-tailed t-test. Single asterisks (*) indicate significantly higher results from no neural data, $r = 0$, at $p < .05$ on a one-tailed t-test. Chance accuracy is indicated by dashed black lines in A. Shaded areas and vertical bars on plot are \pm SEM over 10 different random initializations of each model.

A.3 The Details of the Teacher Representation Matter

In section 3.3, we compared neural networks trained with different teacher RSMs. For those experiments, we used the optimal cost function weighting ratio, r , found from our experiments with the real V1 RSM: $r = 0.1$. Those experiments showed that, as the teacher RSM better approximated the monkey V1 RSM, the trained neural network achieved better performance. This left open the question of whether training the networks with our randomized "control" RSMs, with different weighting ratios (i.e., not $r = 0.01$) would lead to better performance.

To address this question, we repeated our experiments with other weighting ratios: $r = 0.01$ and $r = 1.0$. We found that, for all RSMs, the best performance was found with $r = 0.01$ (the one used in Sec. 3.3): compare values in Fig. 4 and Fig. A.3.

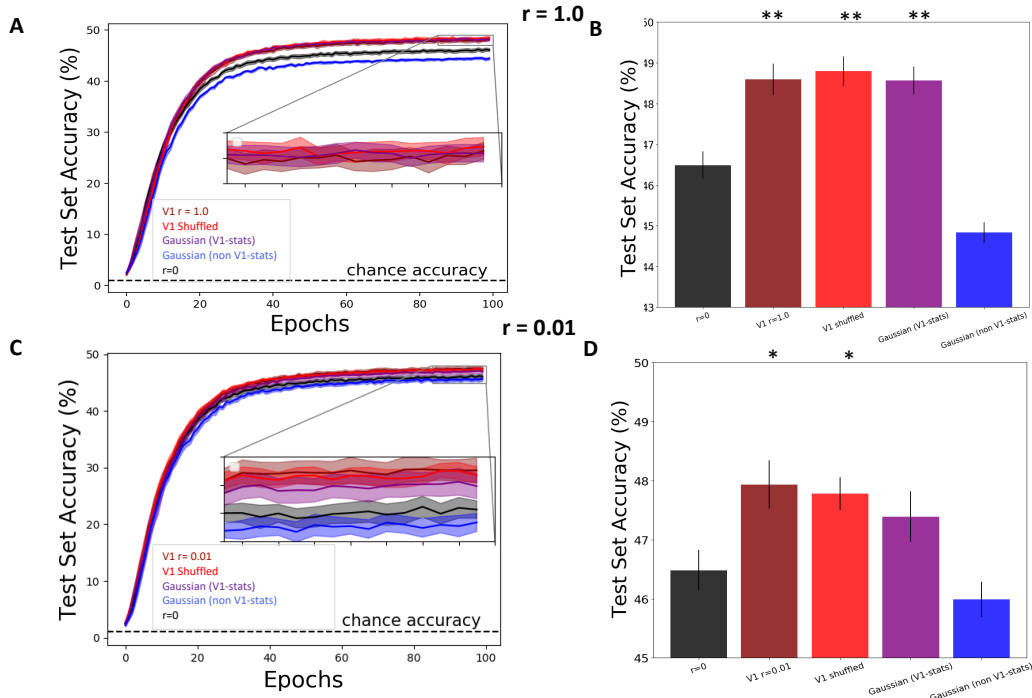


Figure A.3: Accuracy in categorizing previously un-seen CIFAR100 images for networks trained with different teacher RSMs: the real monkey V1 RSM (dark red); V1 shuffled RSM (light red); RSM from random Gaussian vectors drawn with the same mean and standard deviation as the V1 data (Gaussian V1-stats in purple); and RSM from random Gaussian vectors drawn with different mean than the neural data (Gaussian non V1-stats in blue). These were all trained with a weighting of $r = 1.0$ (top panel) and $r = 0.01$ (bottom panel) applied to the representational similarity in the loss function. For comparison, the baseline network (trained with no representational similarity cost) is shown in black. A) and C) Testing accuracy over epochs of training. Shaded areas on plot are \pm SEM over 10 different random initializations of each model. B) and D) Test accuracy plotted (same as in A) by type of data used in forming the teacher RSM. Lines on bars are \pm SEM over 10 different random initializations of each model. Double asterisks (**) indicate significantly higher results from no neural data, $r = 0$, at $p < .001$ on a one-tailed t-test. Single asterisks (*) indicate significantly higher results from no neural data, $r = 0$, at $p < .05$ on a one-tailed t-test.

A.4 The Layer of Representation Teaching Matters

We trained CORNet-Z architecture DCNNs on our composite task, and used the monkey V1 RSM as a teacher for either the V4, or the IT-like areas of CORNet-Z (see Fig. 1 for correspondence between layers). Training the V4-like CORNet-Z layer to mimic monkey V1 led to slightly worse results than training with no teacher RSM ($r = 0$ in black) (Fig. A.4). Training the IT-like layer of CORNet-Z to mimic monkey V1 led to much lower performance (Fig. A.4). This demonstrates that the use of V1 representations as a teacher for the V1-like layer of the neural network is important for performance improvements.

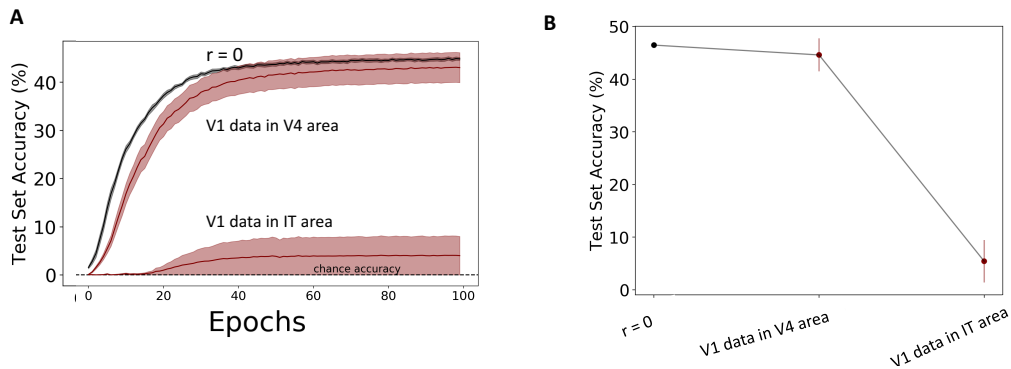


Figure A.4: Accuracy in categorizing previously-unseen CIFAR100 images for the CORNet-Z architecture trained with V1 data in the V4-like area of the CORNet-Z model (top red line) and V1 data in IT-like area of the CORNet-Z model (bottom red line) with $r = 0.1$. A) Test-set accuracy at each epoch during training. Chance accuracy indicated by dashed black line. Shaded areas are \pm SEM over 10 different random initializations of each model. B) Test-set accuracy for previously-unseen CIFAR100 images at the end of training, as a function of neural representation area and weighting.

Acknowledgments

JZ is an Associate Fellow of CIFAR, in the Learning in Machines and Brains Program. JZ further acknowledges the following funding sources: Sloan Fellowship, Canada Research Chairs Program, and Natural Science and Engineering Research Council of Canada (NSERC). CF was supported by an NSF Graduate Research Fellowship, Award #1553798. AF is a Fellow of CIFAR program for Learning in Machines and Brains, and holds a Canada CIFAR AI Chair. AF and HX are funded through CIFAR and an NSERC Discovery Grant.

References

- [1] S.A. Cadena, G.H. Denfield, E.Y. Walker, L.A. Gatys, A.S. Tolias, M. Bethge, and A.S. Ecker. Deep convolutional models improve predictions of macaque V1 responses to natural images. *bioRxiv*, 2017.
- [2] R. Coen-Cagli, A. Kohn, and O. Schwartz. Flexible gating of contextual influences in natural vision. *Nat. Neuro.*, 2015.
- [3] X. Glorot and Y. Bengio. Understanding the difficulty of training deep feedforward neural networks. *J Mach Learn Res*, 2010.
- [4] U. Gu and M.A.J. van Gerven. Deep Neural Networks Reveal a Gradient in the Complexity. *J. Neurosci.*, 2015.
- [5] G. Hinton, O. Vinyals, and J. Dean. Distilling the Knowledge in a Neural Network. *arXiv*, 2015.
- [6] D.H. Hubel and T.N. Wiesel. Receptive Fields and Functional Architecture of Monkey Striate Cortex. *J Physiol.*, 1968.
- [7] W. Kindel, E. Christensen, and J. Zylberberg. Using deep learning to probe the neural code for images in primary visual cortex. *J. Vis.*, 2019.
- [8] N. Kriegeskorte. Deep Supervised, but Not Unsupervised, Models May Explain IT Cortical Representation. *PLOS*, 2014.
- [9] N. Kriegeskorte, M. Mur, and P. Bandettini. Representational similarity analysis – connecting the branches of systems neuroscience. *Front Syst Neurosci.*, 2008.
- [10] A. Krizhevsky and G. Hinton. ImageNet Classification with Deep Convolutional Neural Networks. *NIPS*, 2015.
- [11] Alex Krizhevsky. Learning multiple layers of features from tiny images. Technical report, 2009.
- [12] J. Kubilius, M. Schrimpf, A. Nayebi, D. Bear, D.L.K Yamins, and J.J. Dicarlo. CORnet : Modeling the Neural Mechanisms of Core Object Recognition. *bioRxiv*, 2018.

- [13] Y. Lecun, Y. Bengio, and G. Hinton. Deep Learning. *Nature*, 2015.
- [14] P. Mcclure and N. Kriegeskorte. Representational Distance Learning for Deep Neural Networks. *Front. in Comp. Neuro.*, 2016.
- [15] R. Rajalingham, E.B. Issa, P. Bashivan, K. Kar, K. Schmidt, and J.J. Dicarlo. Large-Scale , High-Resolution Comparison of the Core Visual Object Recognition Behavior of Humans , Monkeys , and State-of-the-Art Deep Artificial Neural Networks. *J. Neurosci.*, 2018.
- [16] A. Romero, N. Ballas, S.E. Kahou, and A. Chassang. FitNets: Hints for Thin Deep Nets. *ICLR*, 2015.
- [17] K. Simonyan and A. Zisserman. Very deep convolutional networks for large-scale image recognition. *ICLR*, 2015.
- [18] N. Srivastava, G. Hinton, A. Krizhevsky, I. Sutskever, and R. Salakhutdinov. Dropout: A simple way to prevent neural networks from overfitting. *J Mach Learn Res*, 2014.
- [19] L. van der Maaten and G. Hinton. Visualizing Data using t-SNE. *J. Mach. Learn. Res.*, 2008.
- [20] D.L.K. Yamins and J.J. Dicarlo. Using goal-driven deep learning models to understand sensory cortex. *Nat. Neuro.*, 2016.